A Fast Globally Optimal Seamline Detection Method for High-Resolution Remote Sensing Images

Huanfeng Shen, *Senior Member, IEEE*, Wei Zhou, and Xinghua Li, *Senior Member, IEEE*

***Abstract*— Seamline detection is one of the most important issues in mosaicking high-resolution remote sensing images (HRRSIs). However, it is difficult to make a balance between efficiency and accuracy. On that account, a shortest matrix path-based dynamic programming (SMP-DP) algorithm is proposed to find the optimal seamline for HRRSI mosaicking. First, a pixel cost matrix defined by intensity difference, gradient similarity, and geometric difference is constructed in the overlapping area. Second, the least average path cost from the starting pixel to each pixel is calculated and the SMP-DP algorithm is applied to find the optimal path. Experimental results on HRRSI prove that the proposed method detects high-quality seamline and crosses much fewer objects with the highest computational efficiency, compared with the state-of-the-art method and commercial software.**

***Index Terms*— Dynamic programming (DP), high-resolution remote sensing images (HRRSIs), image mosaicking, seamline detection, shortest matrix path.**

I. Introduction

With the development of remote sensing technology, high-resolution remote sensing images (HRRSIs) have gradually become the primary source for rapid acquisition of geographic information data [1], [2]. However, the narrow geographic range within a single image cannot meet the requirements of remote sensing applications for large areas. Therefore, it is necessary to stitch a number of HRRSI into one single image with a wider field of view. When mosaicking HRRSI, seamline detection, also known as seamline determination or seam cutting, has an important impact on the quality of the final mosaic [3].

In recent years, a large number of seamline detection methods have been proposed. They aim to find the optimal seamline, where the images show the most intensity and texture similarity [4]. The representative methods include twin-snake model, Dijkstra's algorithm (DA), the dynamic programming (DP) algorithm, and graph cuts (GCs)-based methods. Twin-snake model [5] is a classical seamline detection method in high color and texture similarity areas. There are also many variants on the popular DA [6]. Chon et al. [7] applied DA by limiting the level of maximum difference along seamline. DA was further optimized based on image segmentation [3] and region change rate (RCR) [8]. The DP [9] algorithm also attracts a lot of attention for seamline detection. Wen and Zhou [10] combined DP and gray relational analysis to detect the optimal seamline. An automatic piecewise DP (APDP) method [11] with five search directions was proposed to select the seamline. Recently, GC [12], [13] has been widely used in this field. A novel foreground segmentation-based approach [14] was proposed to detect the optimal seamline for orthoimage mosaicking. Yuan et al. [15] designed a superpixel-based energy function for optimal seamline detection by integrating color difference, gradient difference, and texture complexity information and applied GC. In addition, a new method of seamline determination based on road probability map from the D-LinkNet for urban image mosaicking was presented in [16].

The above methods have their own advantages in different aspects. However, it is difficult to make a tradeoff between efficiency and effectiveness in the optimal seamline detection. For example, although some methods can detect the globally optimal seamline, the efficiency of which are a little low for remote sensing images. The traditional DP methods have significant superiority of the rapid detection, but the selected seamline is usually not globally optimal. This is because traditional DP methods only detect a part of seamlines along three search directions from the first row of pixels and then select the optimal seamline from them. Toward this end, a novel shortest matrix path-based DP (SMP-DP) algorithm is proposed for the efficient and effective seamline detection from HRRSI. Our proposed method detects all seamlines in the matrix along four search directions from one endpoint to another endpoint to find the globally optimal one. The main contributions are as follows.

1) Inspired by the shortest path problem in matrix, the proposed method transforms optimal seamline detection into a path-seam issue from starting point to endpoint in the overlapping area. Therefore, the detected optimal seamline is globally optimal.
2) SMP-DP method not only takes intensity difference, gradient similarity, and geometric difference into account

Manuscript received 7 December 2022; revised 8 February 2023; accepted 23 February 2023. Date of publication 28 February 2023; date of current version 10 March 2023. This work was supported by the Open Fund of Hubei Luojia Laboratory under Grant 220100041 and Grant 220100055. *(Corresponding author: Xinghua Li.)*

Huanfeng Shen is with the School of Resource and Environmental Sciences, Wuhan University, Wuhan 430079, China, and also with the Hubei Luojia Laboratory, Wuhan 430079, China (e-mail: shenhf@whu.edu.cn).

Wei Zhou is with the School of Resource and Environmental Sciences, Wuhan University, Wuhan 430079, China (e-mail: rs_zhouwei@whu.edu.cn).

Xinghua Li is with the School of Remote Sensing and Information Engineering, Wuhan University, Wuhan 430079, China, and also with the Hubei Luojia Laboratory, Wuhan 430079, China (e-mail: lixinghua5540@whu.edu.cn).

Digital Object Identifier 10.1109/LGRS.2023.3250519

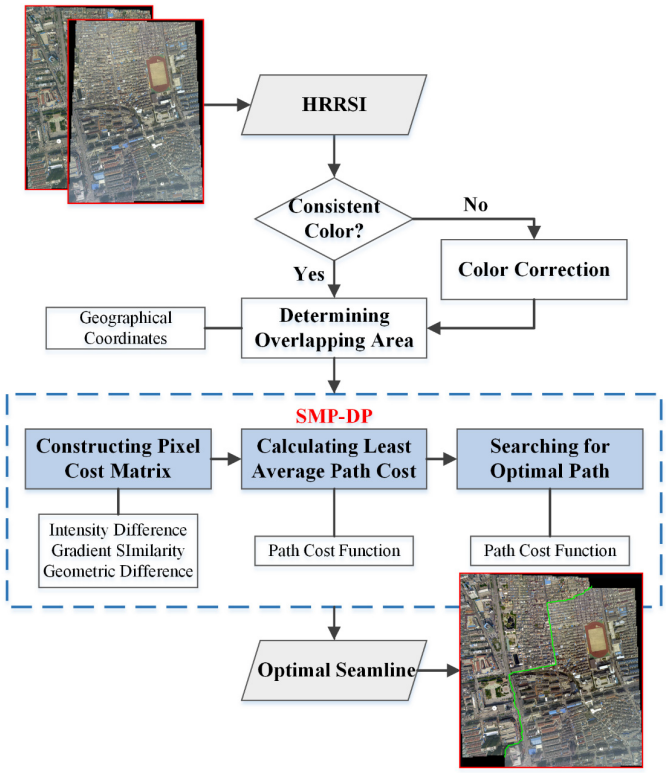

Fig. 1. Flowchart of the proposed seamline detection for HRRSI.

but also inherits the advantages of the traditional DP methods for rapid detection.

The rest of this letter is organized as follows. Section II provides a detailed description on our proposed SMP-DP method for seamline detection. The experimental results are presented in Section III, and the conclusions are made in Section IV.

II. Methods

As we all know, a high-quality seamline should pass through the most similar part in the overlapping area of two images to result in the least inconsistency. A short segment of seamline with significant mismatch is more visible than a lengthy one with small differences [7]. Based on the shortest path problem in matrix, the optimal seamline detection can be regarded as finding a path with the least average cost in the overlapping area. Fig. 1 shows the flowchart of our proposed seamline detection method for HRRSI. It is worth mentioning that if the color differences between two images are too obvious, it is essential to perform color correction [17], [18] before seamline detection. The cost function is calculated by intensity difference, gradient similarity, and geometric difference. Each pixel with a different cost forms a pixel cost matrix. Then, SMP-DP algorithm is applied to detect the optimal seamline in the overlapping area of two images.

A. Shortest Path Problem in Matrix

The shortest path problem in matrix is a classical problem in route planning. It can be described as follows: Given an $n \times m$ matrix with nonnegative elements, it is to find a path from the upper left corner to the lower right corner, so that the sum of the elements on the path is the smallest. The search direction can only be right or down, and the search distance can only be one element.

Inspired by it, we can transform optimal seamline detection into the shortest path problem in matrix. Then, we can detect a globally optimal seamline as the shortest path. An $n \times m$ cost matrix is composed of pixels in the overlapping areas of adjacent images. n and m represent the height and the width of the overlapping areas, respectively. Each pixel has a nonnegative cost and high-cost pixels should be excluded by the optimal seamline. Since a long section of seamline with low cost shows better consistency than a short one with high cost, the shortest path problem is further transformed into finding the path with the least average cost. Different from three search directions of traditional DP methods, the search direction can be expanded to four directions according to the overlapping relationship.

B. Cost Function

The cost function is set to construct the pixel cost matrix and the cost of each pixel reflects the similarity between the overlapping areas of two images. According to Duplaquet's criteria [9], the intensity difference of pixels on the optimal seamline and the geometric difference along the optimal seamline is minimal. In this letter, the intensity difference, gradient similarity, and geometric difference are imposed to calculate the cost function. For two images I_f and I_g, the cost function $C(x, y)$ is defined as

$$C(x, y) = C_d(x, y) + \alpha C_e(x, y) + \beta C_k(x, y) \tag{1}$$

where (x, y) denotes the pixel located at (x, y), and $C_d(x, y)$, $C_e(x, y)$, and $C_k(x, y)$ represent the intensity difference, gradient similarity, and geometric difference of the pixel (x, y), respectively. α and β are the adjustable parameters between intensity difference, gradient similarity, and geometric difference. Empirically, α and β are set to 1.0 in the experiment.

Since HSI color space (H refers to hue, S denotes saturation, and I denotes intensity) is more in line with human visual characteristics than red, green, blue (RGB) color space, its brightness and chromaticity are separable. The intensity difference $C_d(x, y)$ of the pixel (x, y) is computed in the HSI color space, which is defined as

$$C_d(x, y) = \left| I_f^{\mathrm{HSI}}(x, y) - I_g^{\mathrm{HSI}}(x, y) \right| \tag{2}$$

where $I_f^{\mathrm{HSI}}(x, y)$ and $I_g^{\mathrm{HSI}}(x, y)$ denote the intensities of the pixel (x, y) of I_f and I_g in HSI color space, respectively. $|\cdot|$ represents the absolute value.

$C_e(x, y)$ represents the gradient similarity between the pixel (x, y) and four adjacent pixels (x_m, y_m) in the search directions, which is defined as

$$C_e(x, y) = \sum_{m=1}^{4} \mathrm{Min}\left(\mathrm{grad}_f(x_m, y_m), \mathrm{grad}_g(x_m, y_m)\right) \tag{3}$$

where $\mathrm{grad}_f(x_m, y_m)$ and $\mathrm{grad}_g(x_m, y_m)$ are the first-order gradients between the pixel (x, y) and the next adjacent pixel

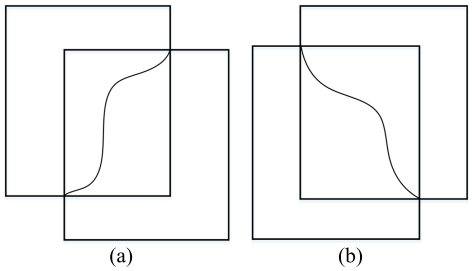

Fig. 2. Overlapping relationship between the two images. (a) Upper left - lower right. (b) Lower left - upper right.

(x_m, y_m) in I_f and I_g, respectively. m denotes the search direction and $\mathrm{Min}(a, b)$ represents the smaller one between a and b.

The geometric difference $C_k(x, y)$ of each pixel is calculated by an eight-direction Sobel gradient operator to detect the edge information, which is defined as

$$C_k(x, y) = \sum_{t=1}^{8} |G_t(x, y)| \tag{4}$$

$$G_t(x, y) = \sum_{n=1}^{3} (f^n(x, y) - g^n(x, y)) \times S_t \tag{5}$$

where $G_t(x, y)$ is the Sobel gradient of the pixel (x, y) in the tth-direction. $f^n(x, y)$ and $g^n(x, y)$ denote the intensity of the pixel (x, y) in the nth band of I_f and I_g in RGB color space, respectively. S_t is the Sobel operator used in the eight directions [19].

C. SMP-DP Algorithm for Seamline Detection

After constructing the cost matrix for pixels in the overlapping area, SMP-DP is applied to find the optimal seamline. The globally optimal seamline is a path from the starting pixel to the end pixel with the least average cost. $C(x, y)$ and $\mathrm{PC}(x, y)$ represent the cost of the pixel (x, y) and the least average cost of the path from the starting pixel to the pixel (x, y), respectively. $L(x, y)$ represents the length of the optimal path from the starting pixel to the pixel (x, y). In fact, SMP-DP is slightly different in the search direction depending on the overlapping relationship of adjacent images. There are usually two main overlapping relationships for the images of the same sensor in Fig. 2, so do other cases. In this letter, our proposed method is presented as in Fig. 2(a).

The SMP-DP algorithm is detailed as follows.

1) According to the overlapping relationship between two images, we determine the upper right pixel as the starting pixel and the lower left pixel as the end pixel of the seamline in the overlapping area.
2) Detect the optimal path from the starting pixel to each pixel (x, y) in turn. For convenience, $F(x+i, y+j)$ is introduced to simplify the formula

$$F(x+i, y+j) = \frac{PC(x+i, y+j) + C(x, y)}{L(x+i, y+j) + 1} \tag{6}$$

where $F(x+i, y+j)$ denotes the cost of the optimal path from the starting pixel to the pixel (x, y) passing through the pixel $(x+i, y+j)$. $L(x+i, y+j)$ represents the length of the optimal path from the starting pixel to the pixel $(x+i, y+j)$.

3) First of all, each pixel in the first row can only be detected by the pixel to its right. So, $\mathrm{PC}(x, y)$ is defined as

$$\mathrm{PC}(x, y) = F(x, y+1). \tag{7}$$

4) Pixels in the last column can be detected by the upper left and upper pixels. $\mathrm{PC}(x, y)$ is defined as

$$\mathrm{PC}(x, y) = \mathrm{Min}(F(x-1, y-1), F(x-1, y)). \tag{8}$$

5) Pixels in the first column can be detected by the upper, upper right, and right pixels. $\mathrm{PC}(x, y)$ is defined as

$$\mathrm{PC}(x, y) = \mathrm{Min}(F(x-1, y), F(x-1, y+1), F(x, y+1)). \tag{9}$$

6) The remaining pixels are detected by the pixels in the upper left, upper, upper right, and right. $\mathrm{PC}(x, y)$ is defined as

$$\mathrm{PC}(x, y) = \mathrm{Min}(F(x-1, y-1), F(x-1, y), F(x-1, y+1)F(x, y+1)). \tag{10}$$

7) Since $\mathrm{PC}(0, \mathrm{width}-1) = C(0, \mathrm{width}-1)$ and each $C(x, y)$ is known, each $\mathrm{PC}(x, y)$ can be calculated in the matrix. Obviously, we can get $\mathrm{PC}(\mathrm{height}-1, 0)$, which represents the least average cost of the path from the starting pixel to the end pixel. Then, we can start from the end pixel $(\mathrm{height}-1, 0)$ to search for the previous pixel in turn by reversing formulas (6)–(10).
8) Connecting all pixels from pixel $(\mathrm{height}-1, 0)$ to pixel $(0, \mathrm{width}-1)$ in sequence, we can find a path from the end pixel to the starting pixel, which is the globally optimal seamline in the overlapping area.

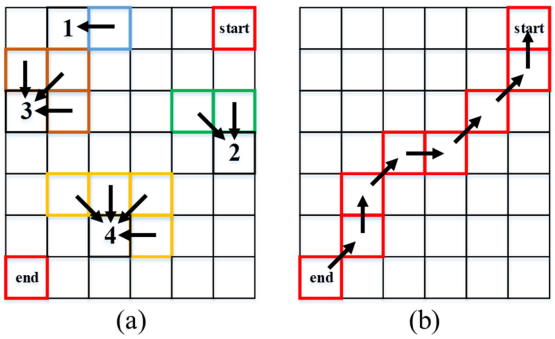

Fig. 3. (a) Different search directions of pixels. (b) Process of searching for the globally optimal seamline.

Fig. 3(a) shows different search directions of pixels in different areas of the matrix. Pixels 1–4 represent the pixel located in the first row, last column, first column, and the middle, respectively. Fig. 3(b) shows the process of the globally optimal seamline detection. It can be seen that the globally optimal seamline is determined from the end pixel to the previous pixel until the starting pixel.

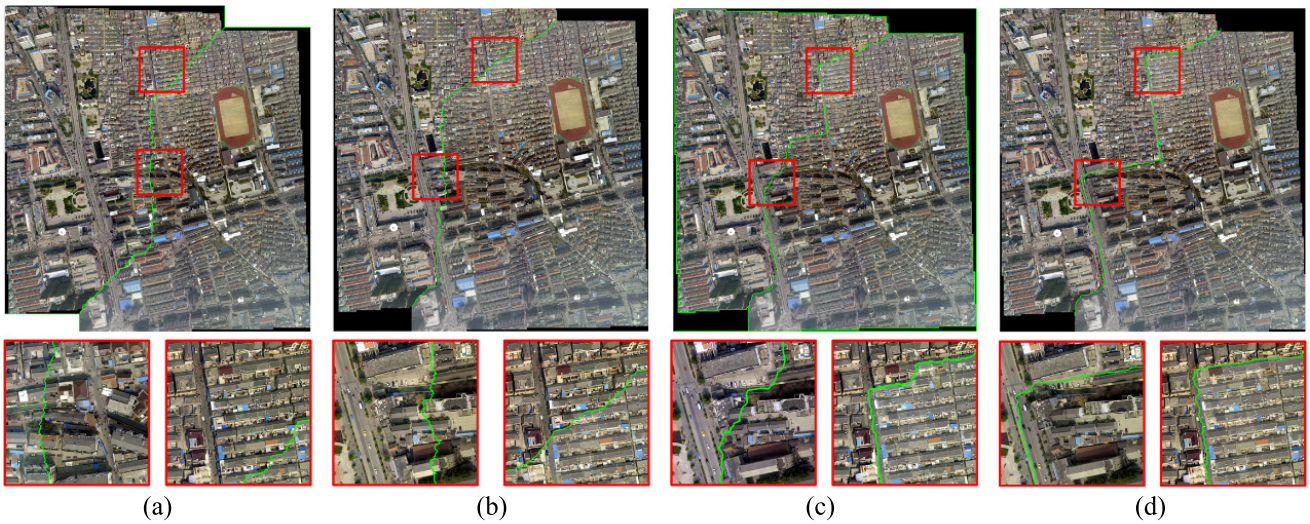

Fig. 4. Visual judgment of the optimal seamline detected by (a) ERDAS, (b) APDP, (c) OrthoVista, and (d) SMP-DP on the first dataset.

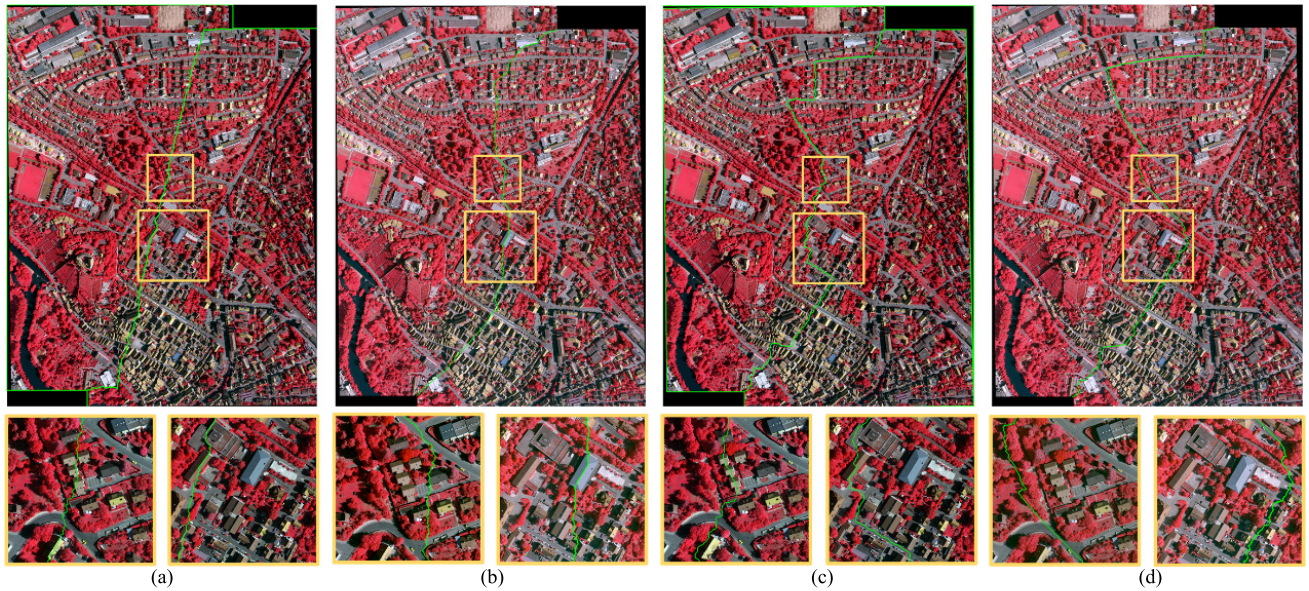

Fig. 5. Visual judgment of the optimal seamline detected by (a) ERDAS, (b) APDP, (c) OrthoVista, and (d) SMP-DP on the second dataset.

III. Experimental Results

Two sets of HRRSI are employed to validate the proposed method. The first dataset is aerial images from an urban area with a ground resolution of 0.1 m, and the spectral bands are infrared, red, and green. The sizes of the two aerial images are 6401 × 8951 and 6701 × 8851, respectively. The buildings in aerial images are apparently oblique. The second dataset is selected from the Vaihingen[1] dataset with the resolution of 0.1 m, and the spectral bands are red, green, and blue. The sizes of the two aerial images are 7680 × 13 270 and 7830 × 13 017, respectively. There are many individual buildings and trees surrounding the buildings in the images. It is worth noting that these two datasets are not orthoimages, and the first dataset has been color corrected by Global Tilting Adjustment in OrthoVista.[2]

[1]https://www2.isprs.org/commissions/comm2/wg4/benchmark/2d-sem-label-vaihingen/

[2]http://www.trimble.com/

To verify the effectiveness and efficiency of our proposed method, we compared SMP-DP with APDP [9] and two commercial software OrthoVista and ERDAS in terms of visual judgment and quantitative assessment.

A. Visual Judgment

Fig. 4 shows the optimal seamline detected by different methods on the first data set. Some details of the red box are shown in the small grid in the following. The fewer buildings the optimal seamline passes through, the better the result. It can be clearly seen that the optimal seamline detected by SMP-DP successfully avoids going through buildings and maintains the consistency and continuity of aerial images. APDP, OrthoVista, and ERDAS cross many buildings and cause significant dislocations, as shown in Fig. 4(b)–(d), especially in the enlarged red box. In addition, SMP-DP always detects and takes full advantage of the road to generate the seamline in the first dataset with many oblique buildings. However, APDP only bypasses the building well in the middle

TABLE I
QUANTITATIVE COMPARISON WITH DIFFERENT METHODS

Datasets	Methods	Numbers of obvious objects passed through	Times(s)
Dataset 1	ERDAS	40+ buildings	19.00
	APDP	20 buildings	30.79
	OrthoVista	11 buildings	16.00
	SMP-DP	**3 buildings**	**6.42**
Dataset 2	ERDAS	21 buildings	60.00
	APDP	16 buildings	75.84
	OrthoVista	8 buildings	79.00
	SMP-DP	**2 buildings**	**12.68**

section and crosses many buildings in the upper and lower sections. OrthoVista detects the seamline along the road in most cases, but performs poorly in densely distributed buildings. The results of ERDAS are relatively poor and pass through the most buildings compared with other methods. Fig. 5 shows the results of the above four methods on the second dataset. SMP-DP can make the seamline along the road and avoid dense buildings and trees. The other three methods inevitably cross a number of buildings. Notably, since these two datasets are not completely aligned, our method will also pass through the building in some area, where other methods pass through the building. From the above experiments, we can draw the conclusion that SMP-DP can generate a high-quality seamline, which passes through a flat area and bypass the buildings and trees.

B. Quantitative Assessment

A quantitative comparison was made to further prove the effectiveness and efficiency of our method. As shown in Table I, it is obvious from the third column that our proposed SMP-DP method passes through much fewer obvious objects than other methods. SMP-DP is very robust on different datasets, only passing through a very small number of buildings. Both OrthoVista and APDP pass through quite a few buildings. ERDAS goes through the largest number of buildings and is the least robust. It can be seen that our proposed SMP-DP method has significantly reduced time cost compared with other three methods. SMP-DP only takes 6 s on the first dataset and 12 s on the second dataset. It is three to five times more efficient than other three methods. This is mainly because DP algorithms have lower time complexity than other algorithms. In addition, different from traditional DP methods to find the optimal seamline from all the pixels in the first row, our proposed method only needs to start from a vertex pixel to detect the optimal seamline, which saves more time.

IV. CONCLUSION

In this letter, we proposed an efficient and effective seamline detection method for HRRSI via a novel SMP-DP algorithm. Referring to the shortest path problem in matrix, a pixel cost matrix that considers intensity difference, gradient similarity, and geometric difference is constructed in the overlapping area. Then, the least average cost of the path from the starting pixel to each pixel is determined. Finally, SMP-DP algorithm is applied to find the optimal seamline with different search directions. By comparing with state-of-the-art method and two kinds of commercial software, it can be proved that our proposed method gets the highest quality seamline in the shortest time. Moreover, if HRRSI is well registered, the result of the mosaic will be better. Color correction is also a very important part of image mosaicking. In the future, we will focus on applying our method to multiple HRRSI mosaicking.

REFERENCES

[1] Y. Cheng, S. Jin, M. Wang, Y. Zhu, and Z. Dong, "A new image mosaicking approach for the multiple camera system of the optical remote sensing satellite GaoFen1," *Remote Sens. Lett.*, vol. 8, no. 11, pp. 1042–1051, Jul. 2017.

[2] Y. Ye, J. Shan, S. Hao, L. Bruzzone, and Y. Qin, "A local phase based invariant feature for remote sensing image matching," *ISPRS J. Photogramm. Remote Sens.*, vol. 142, pp. 205–221, Aug. 2018.

[3] J. Pan, Q. Zhou, and M. Wang, "Seamline determination based on segmentation for urban image mosaicking," *IEEE Geosci. Remote Sens. Lett.*, vol. 11, no. 8, pp. 1335–1339, Aug. 2014.

[4] X. Li, R. Feng, X. Guan, H. Shen, and L. Zhang, "Remote sensing image mosaicking: Achievements and challenges," *IEEE Geosci. Remote Sens. Mag.*, vol. 7, no. 4, pp. 8–22, Apr. 2019.

[5] M. Kerschner, "Seamline detection in colour orthoimage mosaicking by use of twin snakes," *ISPRS J. Photogramm. Remote Sens.*, vol. 56, no. 1, pp. 53–64, Jun. 2001.

[6] J. Davis, "Mosaics of scenes with moving objects," in *Proc. IEEE Comput. Soc. Conf. Comput. Vis. Pattern Recognit.*, Jun. 1998, pp. 354–360.

[7] J. Chon, H. Kim, and C. S. Lin, "Seam-line determination for image mosaicking: A technique minimizing the maximum local mismatch and the global cost," *ISPRS J. Photogramm. Remote Sens.*, vol. 65, no. 1, pp. 86–92, 2010.

[8] J. Pan, M. Wang, J. Li, S. Yuan, and F. Hu, "Region change rate-driven seamline determination method," *ISPRS J. Photogramm. Remote Sens.*, vol. 105, pp. 141–154, Jul. 2015.

[9] M.-L. Duplaquet, "Building large image mosaics with invisible seam lines," in *Proc. SPIE*, 1998, pp. 369–377.

[10] H. Wen and J. Zhou, "An improved algorithm for image mosaic," in *Proc. Int. Symp. Inf. Sci. Eng.*, 2008, pp. 497–500.

[11] X. Li, N. Hui, H. Shen, Y. Fu, and L. Zhang, "A robust mosaicking procedure for high spatial resolution remote sensing images," *J. Photogramm. Remote Sens.*, vol. 109, pp. 108–125, Nov. 2015.

[12] L. Li, J. Yao, R. Xie, and J. Li, "Edge-enhanced optimal seamline detection for orthoimage mosaicking," *IEEE Geosci. Remote Sens. Lett.*, vol. 15, no. 5, pp. 764–768, May 2018.

[13] L. Li, J. Yao, X. Lu, J. Tu, and J. Shan, "Optimal seamline detection for multiple image mosaicking via graph cuts," *ISPRS J. Photogramm. Remote Sens.*, vol. 113, pp. 1–16, Mar. 2016.

[14] L. Li, J. Tu, Y. Gong, J. Yao, and J. Li, "Seamline network generation based on foreground segmentation for orthoimage mosaicking," *ISPRS J. Photogramm. Remote Sens.*, vol. 148, pp. 41–53, Feb. 2019.

[15] Y. Yuan, F. Fang, and G. Zhang, "Superpixel-based seamless image stitching for UAV images," *IEEE Trans. Geosci. Remote Sens.*, vol. 59, no. 2, pp. 1565–1576, Feb. 2020.

[16] S. Yuan, K. Yang, X. Li, and H. Cai, "Automatic seamline determination for urban image mosaicking based on road probability map from the D-LinkNet neural network," *Sensors*, vol. 20, no. 7, p. 1832, Mar. 2020.

[17] J. Wei, W. Tang, and C. He, "Enblending mosaicked remote sensing images with spatiotemporal fusion of convolutional neural networks," *IEEE J. Sel. Topics Appl. Earth Observ. Remote Sens.*, vol. 14, pp. 5891–5902, 2021.

[18] X. Zhang, R. Feng, X. Li, H. Shen, and Z. Yuan, "Block adjustment-based radiometric normalization by considering global and local differences," *IEEE Geosci. Remote Sens. Lett.*, vol. 19, pp. 1–5, 2022.

[19] C. Xing, J. Wang, and Y. Xu, "An optimal seamline based mosaic method for UAV sequence images," in *Proc. Int. Conf. Civil Environ. Eng.*, 2010.